



Published in final edited form as:

J Am Chem Soc. 2021 December 15; 143(49): 20697–20709. doi:10.1021/jacs.1c08060.

Discovery of di- and trihaloacetamides as covalent SARS-CoV-2 main protease inhibitors with high target specificity

Chunlong Ma^{1,#}, Zilei Xia^{1,#}, Michael Dominic Sacco², Yanmei Hu¹, Julia Alma Townsend³, Xiangzhi Meng⁴, Juliana Choza¹, Haozhou Tan¹, Janice Jang¹, Maura V Gongora², Xiujun Zhang², Fushun Zhang⁴, Yan Xiang⁴, Michael Thomas Marty³, Yu Chen^{2,*}, Jun Wang^{1,*}

¹Department of Pharmacology and Toxicology, College of Pharmacy, The University of Arizona, Tucson, AZ, 85721, United States

*Corresponding Author: **Jun Wang** – Department of Pharmacology and toxicology, College of Pharmacy, University of Arizona, 1703 E. Mabel St, Tucson, AZ, 85721, United States; Phone: +1-520-626-1366; Fax: 520-626-0749, junwang@pharmacy.arizona.edu, **Yu Chen** – Department of Molecular Medicine, Morsani College of Medicine, University of South Florida, 12901 Bruce B. Downs Blvd, Tampa, FL, 33612, United States; Phone: +1-813-974-7809; ychen1@usf.edu.

[#]C. M., and Z. X. contributed equally to this work.

AUTHOR CONTRIBUTIONS

C. M. and Z. X. made equal contribution to this study; J. W., Y.C., and M.S. wrote the manuscript with the input from others.

Chunlong Ma – Department of Pharmacology and Toxicology, College of Pharmacy, The University of Arizona, Tucson, AZ, 85721, United States

Zilei Xia – Department of Pharmacology and Toxicology, College of Pharmacy, The University of Arizona, Tucson, AZ, 85721, United States

Michael Dominic Sacco – Department of Molecular Medicine, Morsani College of Medicine, University of South Florida, Tampa, FL, 33612, United States

Yanmei Hu – Department of Pharmacology and Toxicology, College of Pharmacy, The University of Arizona, Tucson, AZ, 85721, United States

Julia Alma Townsend – Department of Chemistry and Biochemistry, The University of Arizona, Tucson, AZ, 85721, United States

Xiangzhi Meng – Department of Microbiology, Immunology and Molecular Genetics, University of Texas Health Science Center at San Antonio, San Antonio, TX, 78229, United States

Juliana Choza – Department of Pharmacology and Toxicology, College of Pharmacy, The University of Arizona, Tucson, AZ, 85721, United States

Haozhou Tan – Department of Pharmacology and Toxicology, College of Pharmacy, The University of Arizona, Tucson, AZ, 85721, United States

Janice Jang – Department of Pharmacology and Toxicology, College of Pharmacy, The University of Arizona, Tucson, AZ, 85721, United States

Maura V Gongora – Department of Molecular Medicine, Morsani College of Medicine, University of South Florida, Tampa, FL, 33612, United States

Xiujun Zhang – Department of Molecular Medicine, Morsani College of Medicine, University of South Florida, Tampa, FL, 33612, United States

Fushun Zhang – Department of Microbiology, Immunology and Molecular Genetics, University of Texas Health Science Center at San Antonio, San Antonio, TX, 78229, United States

Yan Xiang – Department of Microbiology, Immunology and Molecular Genetics, University of Texas Health Science Center at San Antonio, San Antonio, TX, 78229, United States

Michael Thomas Marty – Department of Chemistry and Biochemistry, The University of Arizona, Tucson, AZ, 85721, United States

Jun Wang – Department of Pharmacology and toxicology, College of Pharmacy, University of Arizona, 1703 E. Mabel St, Tucson, AZ, 85721, United States

Yu Chen – Department of Molecular Medicine, Morsani College of Medicine, University of South Florida, 12901 Bruce B. Downs Blvd, Tampa, FL, 33612, United States

Competing interests

A patent was filed by Jun Wang which claims the potential use of **Jun9-62-2R** and related analogs as COVID-19 antiviral drug candidates.

ASSOCIATED CONTENT

Supporting information

The supporting information is available free of charge at

Additional figures and tables describing the experimental materials, methods, X-ray data set, synthesis and characterization of the M^{pro} inhibitors.

²Department of Molecular Medicine, Morsani College of Medicine, University of South Florida, Tampa, FL, 33612, United States

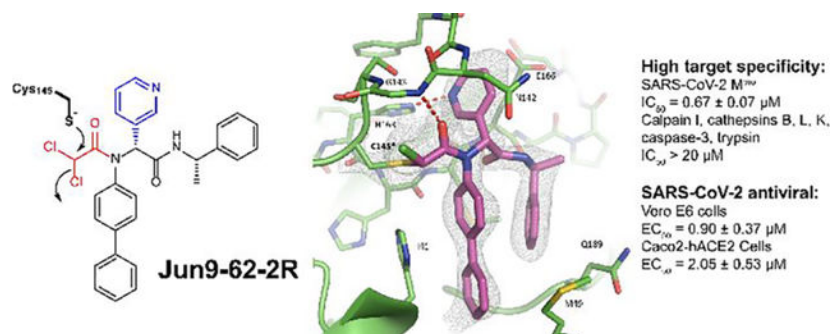
³Department of Chemistry and Biochemistry, The University of Arizona, Tucson, AZ, 85721, United States

⁴Department of Microbiology, Immunology and Molecular Genetics, University of Texas Health Science Center at San Antonio, San Antonio, TX, 78229, United States

Abstract

The main protease (M^{Pro}) is a validated antiviral drug target of SARS-CoV-2. A number of M^{Pro} inhibitors have now advanced to animal model study and human clinical trials. However, one issue yet to be addressed is the target selectivity over host proteases such as cathepsin L. In this study we describe the rational design of covalent SARS-CoV-2 M^{Pro} inhibitors with novel cysteine reactive warheads including dichloroacetamide, dibromoacetamide, tribromoacetamide, 2-bromo-2, 2-dichloroacetamide, and 2-chloro-2, 2-dibromoacetamide. The promising lead candidates **Jun9-62-2R** (dichloroacetamide) and **Jun9-88-6R** (tribromoacetamide) had not only potent enzymatic inhibition and antiviral activity, but also significantly improved target specificity over caplain and cathepsins. Compared to **GC-376**, these new compounds did not inhibit the host cysteine proteases including calpain I, cathepsin B, cathepsin K, cathepsin L, and caspase-3. To the best of our knowledge, they are among the most selective covalent M^{Pro} inhibitors reported thus far. The co-crystal structures of SARS-CoV-2 M^{Pro} with **Jun9-62-2R** and **Jun9-57-3R** reaffirmed our design hypothesis, showing that both compounds form a covalent adduct with the catalytic C145. Overall, these novel compounds represent valuable chemical probes for target validation and drug candidates for further development as SARS-CoV-2 antivirals.

Graphical Abstract



Keywords

SARS-CoV-2; COVID-19; main protease; cysteine warhead; antiviral

INTRODUCTION

The ongoing COVID-19 pandemic is a timely reminder that direct-acting antivirals are urgently needed. Despite the expeditious development of mRNA vaccines, SARS-CoV-2

is likely to remain a significant public health concern in the foreseeable future for several reasons. First, variant viruses with escape mutations continue to emerge, which compromise the efficacy of vaccines.¹ Second, a portion of the population opt out of vaccination based on their religious beliefs, concerns of long-term side effects or other reasons. As such, it is unpredictable when or whether herd immunity can be achieved. Third, the durability of COVID vaccines is currently unknown. Therefore, antivirals are important complements of vaccines to combat both current COVID-19 pandemic and future coronavirus outbreaks.

In combating the COVID-19 pandemic, researchers from different disciplines work relentlessly to discover countermeasures. Drug repurposing led to the identification of remdesivir as the first FDA-approved SARS-CoV-2 antiviral. **EIDD-2801**, another viral polymerase inhibitor discovered through a similar approach, is in human clinical II/III trials.² Among the drug targets exploited, the viral polymerase including the main protease (M^{pro}) and the papain-like protease (PL^{pro}) are the most extensively studied.³ The M^{pro} is a cysteine protease and digests the viral polyprotein at more than 11 sites during the viral replication. M^{pro} functions as a dimer and has a unique preference for glutamine at the substrate P1 position. M^{pro} is a validated high-profile antiviral drug target and M^{pro} inhibitors have demonstrated potent antiviral activity in cell cultures and animal models (Figure 1).⁴⁻⁸ Two Pfizer M^{pro} inhibitors **PF-07304814** and **PF-07321332** are advanced to phase I clinical trial.⁹⁻¹⁰ Additional promising leads are listed in Table 1, which are in different stages of translational development. The success of fast-track development of SARS-CoV-2 M^{pro} inhibitors is a result of accumulated expertise and knowledge in targeting SARS-CoV M^{pro} and similar picornavirus 3C-like (3CL) proteases over the years.¹¹ Despite the tremendous progress in developing M^{pro} inhibitors, the selectivity profiling has thus far been largely neglected. It is essential to address the target selectivity issue early on to avoid catastrophic failures in the later clinical studies. Cysteine protease inhibitor has yet received FDA approval, and the lack of target specificity might be the culprit.

The majority of current reported SARS-CoV-2 M^{pro} inhibitors are peptidomimetic covalent inhibitors with a reactive warhead such as ketone, aldehyde or ketoamide.¹¹ Some of the promising examples include the Pfizer compounds **PF-07304814** (the parent compound **PF-00835231**),¹⁰ **11a**,¹² **GC-376**,^{7, 13} the deuterated **GC-376 (D2-GC-376)**,⁵ **6e**, **6j**,¹⁴ **MI-09**, **MI-30**,⁴ and **MPI8**¹⁵ (Figure 1). Although the high reactivity of these reactive warheads, especially the aldehyde, confers potent activities in the enzymatic assay and antiviral assay, it inevitably leads to off-target side effects through reacting with some host proteins.¹⁶⁻¹⁹ For example, we and others have shown that **GC-376** is a potent inhibitor of cathepsin L (Table 1).^{17, 20} A recent study revealed that **MP18**, an analog of **GC-376** with an aldehyde warhead, inhibits cathepsins B, L, and K with IC_{50} values of 1.2, 230, and 180 nM, respectively.¹⁵ The off-target effect is also a potential concern for some of the most advanced M^{pro} inhibitors including the clinical candidate **PF-07304814**,²¹ compounds **6j** and **6e** which showed *in vivo* antiviral efficacy against MERS-CoV-2 infection in mice,²² and compound **11a** with potent *in vitro* antiviral activity (Table 1).²³ All of these compounds are potent inhibitors of cathepsin L. The high reactivity of the aldehyde warhead might confer the lack of target specificity, and the design of covalent inhibitors with a high target specificity remains a daunting task.

We report herein the rational design of covalent M^{Pro} inhibitors with novel cysteine reactive warheads and high target specificity. Specifically, guided by the X-ray crystal structure of SARS-CoV-2 M^{Pro} with **23R (Jun8-76-3A)** (PDB: 7KX5), which was one of the most potent noncovalent M^{Pro} inhibitors developed from our earlier study,²⁴ we systematically explored a number of novel electrophiles in replacement of the P1' furyl substitution in **23R**. The aim is to identify C145 reactive electrophiles with both potent M^{Pro} inhibition and high target selectivity. This effort led to the discovery of several novel cysteine reactive warheads including dichloroacetamide, dibromoacetamide, tribromoacetamide, 2-bromo-2, 2-dichloroacetamide, and 2-chloro-2, 2-dibromoacetamide. One of the most potent lead compounds **Jun9-62-2R** (dichloroacetamide) inhibited SARS-CoV-2 M^{Pro} with an IC₅₀ of 0.43 μM and viral replication with an EC₅₀ of 2.05 μM in Caco2-hACE2 cells. Significantly, unlike **GC-376**, **Jun9-62-2R** (dichloroacetamide) and **Jun9-88-6R** (tribromoacetamide) are highly selective toward M^{Pro} and do not inhibit the host calpain I, cathepsins B, K, L, caspase-3, and trypsin. X-ray crystal structure of SARS-CoV-2 M^{Pro} with **Jun9-62-2R** (dichloroacetamide) and **Jun9-57-3R** (chloroacetamide) revealed that the C145 forms a covalent adduct with the reactive warheads. Overall, the discovery of these di- and trihaloacetamides as novel cysteine reactive warheads shed light on feasibility of developing SARS-CoV-2 M^{Pro} inhibitors with high target specificity over tested calpain and cathepsins and cellular selectivity index. These novel compounds represent valuable chemical probes for target validation and drug candidates for further development as SARS-CoV-2 antivirals.

RESULTS AND DISCUSSION

Synthesis of covalent M^{Pro} inhibitors.

The covalent M^{Pro} inhibitors were synthesized by the one-pot Ugi four-component reaction (Ugi-4CR) as shown for **Jun9-62-2** (Figure 2) with yields from 33% to 88%. For compounds with potent enzymatic inhibition, the diastereomers were subsequently separated by chiral HPLC. The absolute stereochemistry of **Jun9-57-3R** and **Jun9-62-2R** was determined by X-ray crystallography, and the stereochemistry for the diastereomers of **Jun9-90-4**, **Jun9-89-2**, **Jun9-89-4**, and **Jun9-88-6** were tentatively assigned based on their relevant retention time in chiral HPLC.

Rational design of covalent M^{Pro} inhibitors.

23R was designed based on the superimposed X-ray crystal structure of **GC-376** with **ML188** and **UAWJ254**.²⁴⁻²⁵ The X-ray crystal structure showed that the furyl substitution at the P1' position of **23R** is in close proximity with the catalytic cysteine 145 (3.4 Å between C145 sulfur and the C-2 carbon of furyl, PDB: 7KX5) (Figure 3A), suggesting replacement of furyl with a reactive warhead might lead to covalent inhibitors (Figure 3B). **23R** is an ideal lead candidate for the design of covalent M^{Pro} inhibitors for several reasons: 1) the P1, P2, and P3 substitutions have already been optimized; 2) the designed compounds can be expeditiously synthesized by the one-pot Ugi-4CR; and 3) a diverse of cysteine reactive warheads are commercially available and can be promptly introduced at the P1' position to react with the C145.

Although a number of thiol-reactive warheads have been exploited in the development of covalent protease and kinase inhibitors,^{26–28} we decided to focus on pharmacologically compliant reactive warheads from the FDA-approved drugs. The majority of FDA-approved thiol-reactive drugs are kinase inhibitors including ibrutinib, osimertinib, zanubrutinib, acalabrutinib, dacomitinib, neratinib, and afatinib (Figure 3C).²⁶ As such, acrylamide and 2-butyramide were chosen as reactive warheads in our initial design of covalent SARS-CoV-2 M^{PRO} inhibitors (Figure 3B). Chloroacetamide was also chosen as it was previously explored by Pfizer for the development of SARS-CoV and SARS-CoV-2 M^{PRO} inhibitors (Pfizer compound **12**) (Figure 3C).²¹ Chloroacetamide is frequently used as a reactive warhead for designing chemical probes for target pull down.²⁹ Finally, we included azidomethylene as it was previously shown to be a relatively unreactive cysteine warhead.^{30–31} The fluoroacetamide was included as a control.

The designed covalent SARS-CoV-2 M^{PRO} inhibitors were shown in Figure 3D. All compounds were first tested in the FRET-based M^{PRO} enzymatic assay. Active hits were further tested for cellular cytotoxicity to select candidates for the following antiviral assay against SARS-CoV-2. It was found that the azidoacetamide **Jun9-61-1** and the fluoracetamide **Jun9-61-4** were not active (IC₅₀ > 20 μM). Surprisingly, the acrylamides **Jun10-15-2** and **Jun9-51-3** were also not active (IC₅₀ > 20 μM), suggesting the acrylamide might not be positioned at the right geometry for reacting with the C145. Gratifyingly, **Jun9-62-1** with the 2-butyramide warhead showed potent inhibition with an IC₅₀ of 1.15 μM. However, **Jun9-62-1** also had moderate cytotoxicity in both Vero E6 (CC₅₀ = 17.99 μM) and Calu-3 (CC₅₀ = 47.77 μM) cells. Similarly, covalent inhibitors with the chloroacetamide reactive warhead had potent inhibition against SARS-CoV-2 M^{PRO}. The most potent compound **Jun9-57-3R** inhibited SARS-CoV-2 M^{PRO} with an IC₅₀ of 0.05 μM, comparable to the potency of **GC-376** (IC₅₀ = 0.03 μM). Interestingly, the diastereomer **Jun9-57-3S** was also a potent M^{PRO} inhibitor with an IC₅₀ of 1.13 μM. However, covalent inhibitors with the chloroacetamide warhead **Jun9-54-1**, **Jun9-59-1**, **Jun9-55-2**, **Jun9-57-3R**, **Jun9-57-3S**, **Jun9-57-2**, and **Jun9-55-1** were highly cytotoxic in Vero E6 (CC₅₀ < 11 μM) and Calu-3 (CC₅₀ < 2 μM) cells, possibly due to their off-target effects on host proteins/DNAs. The low cellular selectivity index precludes further development of these covalent M^{PRO} inhibitors as SARS-CoV-2 antiviral drugs.

Exploring acrylamides and haloacetamides as novel warheads for SARS-CoV-2 M^{PRO} C145.

For the acrylamide series of compounds, **Jun9-72-3** and **Jun10-31-4**, both containing a 2-substituted acrylamide warhead, were not active against M^{PRO} (IC₅₀ > 20 μM) (Figure 4). However, compound **Jun10-38-2** with the 2-chloroacrylamide had potent inhibition with an IC₅₀ of 4.22 μM.

For the haloacetamide series of compounds, the reference compound **Jun9-54-1** with the classical chloroacetamide reactive warhead had potent inhibition against SARS-CoV-2 M^{PRO} with an IC₅₀ of 0.17 μM. However, it was cytotoxic in both Vero E6 cells and Calu-3 cells with CC₅₀ values less than 3.5 μM. To increase the cellular selectivity index, we reasoned that substituted chloroacetamides or haloacetamides might have reduced cellular cytotoxicity while maintaining potent M^{PRO} inhibition. It was found that **Jun9-77-1** with the

2-chloropropanamide warhead was not active ($IC_{50} > 20 \mu M$). Encouragingly, compound **Jun9-62-2R** with the dichloroacetamide warhead had potent inhibition against M^{pro} with an IC_{50} of $0.43 \mu M$ while being non-cytotoxic to Vero E6 cells ($CC_{50} > 100 \mu M$). In comparison, the corresponding diastereomer **Jun9-62-2S** was not active ($IC_{50} > 20 \mu M$), which is consistent with the predicted binding mode (Figure 3A). Given these promising results, we further designed two additional dichloroacetamide compounds **Jun9-90-3** and **Jun9-90-4** with variations at the P3/P4 substitutions. Similar to **Jun9-62-2R**, both **Jun9-90-3R** and **Jun9-90-4R** were potent inhibitors with IC_{50} values of 0.30 and $0.46 \mu M$, respectively. Both compounds were also non-cytotoxic to Vero E6 cells ($CC_{50} > 100 \mu M$). In contrast, the corresponding diastereomers **Jun9-90-3S** and **Jun9-90-4S** were not active ($IC_{50} > 20 \mu M$).

We further explored di- and trisubstituted haloacetamides as M^{pro} C145 reactive warheads (Figure 4). **Jun9-89-2R** with the dibromoacetamide warhead is highly active with an IC_{50} of $0.08 \mu M$, however, the cell cytotoxicity also increased ($CC_{50} = 8.94 \mu M$). The diastereomer **Jun9-89-2S** also had potent inhibition against M^{pro} with an IC_{50} of $2.44 \mu M$ and comparable cytotoxicity ($CC_{50} = 4.57 \mu M$). **Jun9-76-4** with the 2, 2-dichloropropanamide warhead, **Jun9-72-4** with the trichloroacetamide, **Jun9-77-2** with the 2-chloro-2, 2-difluoroacetamide were all inactive against M^{pro} ($IC_{50} > 20 \mu M$). **Jun9-89-3** with the 2-bromo-2, 2-dichloroacetamide showed potent inhibition with an IC_{50} of $1.20 \mu M$. The cytotoxicity of **Jun9-89-3** also improved ($CC_{50} = 32.43 \mu M$). **Jun9-89-4R** with the 2-chloro-2, 2-dibromoacetamide warhead is highly potent with an IC_{50} of $0.05 \mu M$, but it was cytotoxic in Vero E6 cells ($CC_{50} = 8.41 \mu M$). The diastereomer **Jun9-89-4S** was less active ($IC_{50} = 9.04 \mu M$). **Jun9-88-6R** with the tribromoacetamide warhead had high potency against M^{pro} with an IC_{50} of $0.08 \mu M$, while the diastereomer **Jun9-88-6S** was less active ($IC_{50} = 7.16 \mu M$). Both **Jun9-88-6R** and **Jun9-88-6S** had comparable cytotoxicity as **Jun9-54-1** with CC_{50} value of 5.48 and $5.99 \mu M$, respectively.

Pharmacological characterization of SARS-CoV-2 M^{pro} inhibitors with novel reactive warheads.

Based on the M^{pro} inhibition and cell cytotoxicity, four compounds **Jun9-62-2R**, **Jun9-90-3R**, **Jun9-90-4R**, and **Jun9-88-6R** were selected for mechanistic studies (Figure 5). Enzymatic kinetic studies suggested that these four compounds bind to M^{pro} in a two-step process: the first step reversible binding (K_I) and the second step irreversible binding (k_{inact}). The calculated k_{inact}/K_I values for **Jun9-62-2R**, **Jun9-90-3R**, **Jun9-90-4R**, and **Jun9-88-6R** were 819.7 , 1543.6 , 867.4 , and $7074.3 M^{-1}s^{-1}$, respectively (Figure 5A). These results were in agreement with the expected mechanism of action in which all four compounds form a covalent bond with the catalytic C145. In the thermal shift-binding assay, all four compounds stabilized the SARS-CoV-2 M^{pro} upon binding as reflected by the T_m shift to higher temperatures (Figure 5B). As the tribromoacetamide is sterically hindered, the mechanism of action of **Jun9-88-6R** might involve the nucleophilic attack of the carbonyl by the C145 thiol to give a thiohemiketal intermediate, followed by a 1,2-shift of the sulfur to displace one bromide (Figure S2).

To provide additional lines of evidence to support the proposed mode of action of covalent binding, we performed three additional experiments. First, to demonstrate the reversibility of the binding of **Jun9-62-2R** to M^{Pro}, we incubated 10 μ M of SARS-CoV-2 M^{Pro} with 10 μ M of **Jun9-62-2R** for 2 h and monitored the enzymatic activity of M^{Pro} following 100-fold dilution of the mixture. It was found that no enzymatic activity was recovered (Figure 5C). In contrast, the mixture with our previously developed non-covalent inhibitor **23R** showed nearly complete recovery of enzymatic activity after dilution (Figure 5C). These results suggest that the binding of **Jun9-62-2R** is irreversible while the binding of **23R** is reversible. Second, we repeated the FRET assay of **Jun9-62-2R** with different pre-incubation times and found that longer pre-incubation time gave lower IC₅₀ values (Figure 5D). This data is consistent with the mode of action of covalent inhibitors.³² In contrast, pre-incubation of M^{Pro} with the non-covalent inhibitor **23R** did not lead to significant changes of the IC₅₀ value (Figure 5D). Third, we used native mass spectrometry to detect the covalent adducts of M^{Pro} with **Jun9-62-2R**, **Jun9-89-2R**, **Jun9-88-6R**, and **Jun9-89-4R**. The expected mass shifts of 482 Da and 526 Da were observed for **Jun9-62-2R** and **Jun9-89-2R**, respectively (Figures 5E and F). Interesting, the expected dibromoacetamide conjugate was not observed for **Jun9-88-6R**, suggesting this conjugate might not be stable. Instead, the mass shift corresponding to the monobromo thiol adduct was observed (Figure 5G). For **Jun9-89-4R**, the mass shifts for both the chlorobromo and chloro thiol adducts were observed (Figure 5H).

To further profile the cellular M^{Pro} inhibition, we tested these four compounds in our recently developed FlipGFP assay.^{18, 33} Briefly, the GFP is split into two parts, the β 1–9 template and the β 10–11 strands. The β 10 and β 11 strands were engineered with K5-E5 linker such that they are restrained in the parallel form. When the linker is cleaved by M^{Pro}, β 10 and β 11 adopt antiparallel conformation, which allows association with the β 1–9 template, leading to the recovery of the GFP signal. In the FlipGFP assay, GFP signal is proportional to the M^{Pro} enzymatic activity. It was found that all four compounds led to dose-dependent inhibition of the GFP signal with EC₅₀ values of 0.96 μ M (**Jun9-62-2R**), 0.91 μ M (**Jun9-90-3R**), 1.57 μ M (**Jun9-90-4R**), and 0.92 μ M (**Jun9-88-6R**) (Figures 5I and J). The EC₅₀ value for the positive control **GC-376** was 1.80 μ M. This result suggests that these four compounds can potentially inhibit the M^{Pro} in the cellular content.

Antiviral activity of SARS-CoV-2 M^{Pro} inhibitors with novel reactive warheads.

The antiviral activity of the four lead compounds was evaluated in both Vero E6 cells and Caco2-hACE2 cells to exclude cell type dependent effect. Caco2-hACE2 with endogenous TMPRSS2 expression is a validated cell line for SARS-CoV-2 antiviral assay.^{34–36} **Jun9-62-2R**, **Jun9-90-3R**, **Jun9-90-4R**, and **Jun9-88-6R** inhibited SARS-CoV-2 replication in Vero E6 cells with EC₅₀ values of 0.90, 2.07, 1.10, and 0.58 μ M, respectively (Figure 6A). All four compounds showed comparable antiviral activity in Caco2-hACE2 cells with EC₅₀ values of 2.05, 3.24, 1.43, and 2.15 μ M, respectively (Figure 6B). In comparison, **GC-376** inhibited SARS-CoV-2 replication in Vero E6 and Caco2-hACE2 cells with EC₅₀ values of 1.51 and 2.90 μ M. When tested in Calu-3 cells, **Jun9-90-3R** showed comparable antiviral activity with an EC₅₀ value of 2.00 μ M (Figure 6C).

Profiling the target selectivity against host proteases.

Lack of target specificity is one of the major reasons that many cysteine protease inhibitors failed in the clinical trials. To profile the target specificity of these SARS-CoV-2 M^{Pro} inhibitors with a novel reactive warhead, we selected **Jun9-62-2R** and **Jun9-88-6R** as representative examples and included the canonical **GC-376** with an aldehyde reactive warhead for comparison. The results showed that **GC-376** had potent inhibition of the host proteases including calpain I, cathepsin B, cathepsin K, and cathepsin L with IC₅₀ values in the submicromolar and nanomolar range. **GC-376** did not inhibit caspase-3 and trypsin (IC₅₀ > 20 μM) (Figure 7). In comparison, both **Jun9-62-2R** and **Jun9-88-6R** had a significantly improved target selectivity and did not show potent inhibition against the host calpain I, cathepsin B, cathepsin K, cathepsin L, caspase-3, and trypsin. **Jun9-88-6R** had weak inhibition against cathepsin L with an IC₅₀ of 7.37 μM, conferring a 94-fold higher selectivity for inhibiting the SARS-CoV-2 M^{Pro}. Collectively, the covalent SARS-CoV-2 M^{Pro} inhibitors **Jun9-62-2R** with the dichloroacetamide warhead and **Jun9-88-6R** with the tribromoacetamide warhead have high target specificity against M^{Pro} over host proteases.

X-ray crystal structures of SARS-CoV-2 M^{Pro} in complex with Jun9-62-2R and Jun9-57-3R.

Using X-ray crystallography we solved the complex structures of SARS-CoV-2 M^{Pro} with **Jun9-57-3R** (2.25 Å, PDB ID 7RN0) and **Jun9-62-2R** (2.30 Å, PDB ID 7RN1) (Figure 8, Table S1). **Jun9-57-3R** and **Jun9-62-2R** have nearly identical chemical features to their non-covalent progenitor **23R (Jun8-76-3A)** (PDB ID 7KX5). As such, the binding poses are very similar. The pyridyl ring binds to the S1 pocket of M^{Pro}, where it forms a hydrogen bond with His163. This hydrogen bond is critical for coordinating the Gln sidechain of its substrate, a residue it is uniquely selective for. Consequently, a hydrogen bond acceptor at this position confers tremendous potency to M^{Pro} inhibitors. The phenylpyrrole (**Jun9-57-3R**) or biphenyl (**Jun9-62-2R**) moieties insert into the hydrophobic S2 pocket where they form nonpolar contacts and stack with the catalytic base, His41. An amide group linking the pyridyl ring to an α-methylbenzene group accepts a hydrogen bond from the mainchain of Glu166. This α-methylbenzene group flips down towards the core of the substrate channel, where it forms additional pi-stacking interactions with the biphenyl or phenylpyrrole moieties. The key distinction between **Jun9-62-2R**, **Jun9-57-3R**, and analogues **Jun8-76-3A** and **ML188** is the presence of an electrophilic chloroacetamide warhead, which forms a covalent adduct with the catalytic cysteine Cys145 (Figure 8C–D). The short distance of this covalent bond (1.8 Å) allows the inhibitor to press further into the oxyanion hole, causing the P2 benzene to rotate inwards by ~ 40°. Likewise, the chloroacetamide warhead is forced towards the catalytic core, causing the P1' chloride of **Jun9-57-3R** to lie closer to Cys145 (2.8 Å) than the corresponding furyl oxygen of **Jun8-76-3A** (3.2 Å).

CONCLUSION

The majority of the reported M^{Pro} inhibitors contain the aldehyde reactive warhead, which is known to have non-specific reactivity towards host proteins.^{16–19} It should be noted that both the Pfizer M^{Pro} inhibitors that are currently in clinical trials do not contain the aldehyde warhead.^{9–10} As such, we are interested in developing SARS-CoV-2 M^{Pro} inhibitors with

high target specificity. A highly specific M^{Pro} inhibitor is also needed for target validation as it separates the effect of M^{Pro} inhibition from host protease inhibition such as cathepsin L. It is known that host cathepsin L is important in SARS-CoV-2 replication in Vero E6 cells, which are TMPRSS2-negative, but not in Calu-3 cells, which are TMPRSS2-positive.³⁷ In this study, we report the discovery of dichloroacetamide, dibromoacetamide, 2-bromo-2, 2-dichloroacetamide, 2-chloro-2, 2-dibromoacetamide, and tribromoacetamide as novel cysteine reactive warheads. To the best of our knowledge, these warheads have not been explored in cysteine protease inhibitors. The most promising lead compounds **Jun9-62-2R** with the dichloroacetamide warhead and **Jun9-88-6R** with the tribromoacetamide inhibited SARS-CoV-2 M^{Pro} with IC₅₀ values of 0.43 μM and 0.08 μM, respectively. These two compounds also showed potent inhibition against SARS-CoV2 in both Vero E6 and Caco2-hACE2 cells with EC₅₀ values in the single-digit to submicromolar range. Significantly, both **Jun9-62-2R** and **Jun9-88-6R** had high target specificity towards M^{Pro} and did not inhibit the host proteases including calpain I, cathepsin B, cathepsin K, cathepsin L, caspase-3, and trypsin. In comparison, GC-376 was not selective and inhibited calpain I, cathepsin B, cathepsin K, and cathepsin L with comparable potency as M^{Pro}. Regarding the translational potential of the di- and trihaloacetamide-containing M^{Pro} inhibitors, the widely used antibiotic chloramphenicol contains the dichloroacetamide, suggesting **Jun9-62-2R** might be tolerated *in vivo*. Follow up studies will optimize the *in vitro* and *in vivo* pharmacokinetic properties and *in vivo* antiviral efficacy of these novel compounds in SARS-CoV-2 infection animal models. Other potential strategies of developing selective M^{Pro} inhibitors including allosteric inhibitors^{38–39} or targeting the more reactive Cys44 at the S2 binding pocket.^{40–41} Overall, these novel compounds represent valuable chemical probes for target validation and promising drug candidates for translational development as SARS-CoV-2 antivirals.

Supplementary Material

Refer to Web version on PubMed Central for supplementary material.

ACKNOWLEDGEMENTS

J. W. was supported by the National Institutes of Health (NIH) (Grants AI158775, AI147325, and AI157046) and the Arizona Biomedical Research Centre Young Investigator grant (ADHS18-198859). We thank Naoya Kitamura for the preliminary work on the synthesis of some of compounds listed in this paper. The antiviral assay in Calu-3 cells was conducted by Drs. David Schultz and Sara Cherry at the University of Pennsylvania through the NIAID preclinical service under a non-clinical evaluation agreement. Y.H. was supported by the T32 GM008804 training grant. We thank Michael Kemp for assistance with crystallization and X-ray diffraction data collection. SBC-CAT is operated by UChicago Argonne, LLC, for the U.S. Department of Energy, Office of Biological and Environmental Research under contract DE-AC02-06CH11357. Y.X. was supported by a COVID-19 pilot grant from UTHSCSA and NIH grant AI151638. SARS-Related Coronavirus 2, Isolate USA-WA1/2020 (NR-52281) was deposited by the Centers for Disease Control and Prevention and obtained through BEI Resources, NIAID, NIH.

REFERENCES

1. Harvey WT; Carabelli AM; Jackson B; Gupta RK; Thomson EC; Harrison EM; Ludden C; Reeve R; Rambaut A; Peacock SJ; Robertson DL; Consortium C-GU, SARS-CoV-2 variants, spike mutations and immune escape. *Nat. Rev. Microbiol.* 2021, 19 (7), 409–424. [PubMed: 34075212]
2. Cox RM; Wolf JD; Plemper RK, Therapeutically administered ribonucleoside analogue MK-4482/EIDD-2801 blocks SARS-CoV-2 transmission in ferrets. *Nat. Microbiol.* 2021, 6 (1), 11–18. [PubMed: 33273742]

3. Morse JS; Lalonde T; Xu S; Liu WR, Learning from the Past: Possible Urgent Prevention and Treatment Options for Severe Acute Respiratory Infections Caused by 2019-nCoV. *Chembiochem* 2020, 21 (5), 730–738. [PubMed: 32022370]
4. Qiao J; Li YS; Zeng R; Liu FL; Luo RH; Huang C; Wang YF; Zhang J; Quan B; Shen C; Mao X; Liu X; Sun W; Yang W; Ni X; Wang K; Xu L; Duan ZL; Zou QC; Zhang HL; Qu W; Long YH; Li MH; Yang RC; Liu X; You J; Zhou Y; Yao R; Li WP; Liu JM; Chen P; Liu Y; Lin GF; Yang X; Zou J; Li L; Hu Y; Lu GW; Li WM; Wei YQ; Zheng YT; Lei J; Yang S, SARS-CoV-2 M(pro) inhibitors with antiviral activity in a transgenic mouse model. *Science* 2021, 371 (6536), 1374–1378. [PubMed: 33602867]
5. Dampalla CS; Zheng J; Perera KD; Wong LR; Meyerholz DK; Nguyen HN; Kashipathy MM; Battaile KP; Lovell S; Kim Y; Perlman S; Groutas WC; Chang KO, Postinfection treatment with a protease inhibitor increases survival of mice with a fatal SARS-CoV-2 infection. *Proc. Natl. Acad. Sci. U. S. A.* 2021, 118 (29), e2101555118. [PubMed: 34210738]
6. Caceres CJ; Cardenas-Garcia S; Carnaccini S; Seibert B; Rajao DS; Wang J; Perez DR, Efficacy of GC-376 against SARS-CoV-2 virus infection in the K18 hACE2 transgenic mouse model. *Sci. Rep.* 2021, 11 (1), 9609. [PubMed: 33953295]
7. Ma C; Sacco MD; Hurst B; Townsend JA; Hu Y; Szeto T; Zhang X; Tarbet B; Marty MT; Chen Y; Wang J, Boceprevir GC-376, and calpain inhibitors II, XII inhibit SARS-CoV-2 viral replication by targeting the viral main protease. *Cell Res.* 2020, 30 (8), 678–692. [PubMed: 32541865]
8. Sacco MD; Ma C; Lagarias P; Gao A; Townsend JA; Meng X; Dube P; Zhang X; Hu Y; Kitamura N; Hurst B; Tarbet B; Marty MT; Kolocouris A; Xiang Y; Chen Y; Wang J, Structure and inhibition of the SARS-CoV-2 main protease reveal strategy for developing dual inhibitors against M(pro) and cathepsin L. *Sci. Adv.* 2020, 6 (50), eabe0751. [PubMed: 33158912]
9. Owen DR; Allerton CMN; Anderson AS; Aschenbrenner L; Avery M; Berritt S; Boras B; Cardin RD; Carlo A; Coffman KJ; Dantonio A; Di L; Eng H; Ferre R; Gajiwala KS; Gibson SA; Greasley SE; Hurst BL; Kadar EP; Kalgutkar AS; Lee JC; Lee J; Liu W; Mason SW; Noell S; Novak JJ; Obach RS; Ogilvie K; Patel NC; Pettersson M; Rai DK; Reese MR; Sammons MF; Sathish JG; Singh RSP; Steppan CM; Stewart AE; Tuttle JB; Updyke L; Verhoest PR; Wei L; Yang Q; Zhu Y An oral SARS-CoV-2 Mpro inhibitor clinical candidate for the treatment of COVID-19. *Science.* 2021, eabl4784.
10. Boras B; Jones RM; Anson BJ; Arenson D; Aschenbrenner L; Bakowski MA; Beutler N; Binder J; Chen E; Eng H; Hammond J; Hoffman R; Kadar EP; Kania R; Kimoto E; Kirkpatrick MG; Lanyon L; Lendy EK; Lillis JR; Luthra SA; Ma C; Noell S; Obach RS; O'Brien MN; O'Connor R; Ogilvie K; Owen D; Pettersson M; Reese MR; Rogers T; Rossulek MI; Sathish JG; Steppan C; Ticehurst M; Updyke LW; Zhu Y; Wang J; Chatterjee AK; Mesecar AD; Anderson AS; Allerton C, Preclinical characterization of an intravenous coronavirus 3CL protease inhibitor for the potential treatment of COVID-19. *Nat. Commun.* 2021, 12(1), 6055. [PubMed: 34663813]
11. Ghosh AK; Brindisi M; Shahabi D; Chapman ME; Mesecar AD, Drug Development and Medicinal Chemistry Efforts toward SARS-Coronavirus and Covid-19 Therapeutics. *ChemMedChem* 2020, 15 (11), 907–932. [PubMed: 32324951]
12. Dai W; Zhang B; Jiang XM; Su H; Li J; Zhao Y; Xie X; Jin Z; Peng J; Liu F; Li C; Li Y; Bai F; Wang H; Cheng X; Cen X; Hu S; Yang X; Wang J; Liu X; Xiao G; Jiang H; Rao Z; Zhang LK; Xu Y; Yang H; Liu H, Structure-based design of antiviral drug candidates targeting the SARS-CoV-2 main protease. *Science* 2020, 368 (6497), 1331–1335. [PubMed: 32321856]
13. Vuong W; Khan MB; Fischer C; Arutyunova E; Lamer T; Shields J; Saffran HA; McKay RT; van Belkum MJ; Joyce MA; Young HS; Tyrrell DL; Vederas JC; Lemieux MJ, Feline coronavirus drug inhibits the main protease of SARS-CoV-2 and blocks virus replication. *Nat. Commun.* 2020, 11 (1), 4282. [PubMed: 32855413]
14. Rathnayake AD; Zheng J; Kim Y; Perera KD; Mackin S; Meyerholz DK; Kashipathy MM; Battaile KP; Lovell S; Perlman S; Groutas WC; Chang KO, 3C-like protease inhibitors block coronavirus replication in vitro and improve survival in MERS-CoV-infected mice. *Sci. Transl. Med.* 2020, 12 (557), eabc5332. [PubMed: 32747425]
15. Yang KS; Ma XR; Ma Y; Alugubelli YR; Scott DA; Vatansever EC; Drelich AK; Sankaran B; Geng ZZ; Blankenship LR; Ward HE; Sheng YJ; Hsu JC; Kratch KC; Zhao B; Hayatshahi HS; Liu J; Li P; Fierke CA; Tseng C-TK; Xu S; Liu WR, A Quick Route to Multiple Highly Potent

SARS-CoV-2 Main Protease Inhibitors**. ChemMedChem 2021, 16 (6), 942–948. [PubMed: 33283984]

16. Ma XR; Alugubelli YR; Ma Y; Vantasever EC; Scott DA; Qiao Y; Yu G; Xu S; Liu WR, MPI8 is Potent against SARS-CoV-2 by Inhibiting Dually and Selectively the SARS-CoV-2 Main Protease and the Host Cathepsin L*. ChemMedChem 2021, doi: 10.1002/cmdc.202100456.
17. Steuten K; Kim H; Widen JC; Babin BM; Onguka O; Lovell S; Bolgi O; Cerikan B; Neufeldt CJ; Cortese M; Muir RK; Bennett JM; Geiss-Friedlander R; Peters C; Bartenschlager R; Bogoy M, Challenges for Targeting SARS-CoV-2 Proteases as a Therapeutic Strategy for COVID-19. ACS Infect. Dis. 2021, 7 (6), 1457–1468. [PubMed: 33570381]
18. Xia Z; Sacco M; Hu Y; Ma C; Meng X; Zhang F; Szeto T; Xiang Y; Chen Y; Wang J, Rational Design of Hybrid SARS-CoV-2 Main Protease Inhibitors Guided by the Superimposed Cocrystal Structures with the Peptidomimetic Inhibitors GC-376, Telaprevir, and Boceprevir. ACS Pharmacol. Transl. Sci. 2021, 4 (4), 1408–1421.
19. Vandyck K; Abdelnabi R; Gupta K; Jochmans D; Jekle A; Deval J; Misner D; Bardiot D; Foo CS; Liu C; Ren S; Beigelman L; Blatt LM; Boland S; Vangeel L; Dejonghe S; Chaltin P; Marchand A; Serebryany V; Stoycheva A; Chanda S; Symons JA; Raboisson P; Neyts J, ALG-097111, a potent and selective SARS-CoV-2 3-chymotrypsin-like cysteine protease inhibitor exhibits in vivo efficacy in a Syrian Hamster model. Biochem. Biophys. Res. Commun. 2021, 555, 134–139. [PubMed: 33813272]
20. Hu Y; Ma C; Szeto T; Hurst B; Tarbet B; Wang J, Boceprevir, Calpain Inhibitors II and XII, and GC-376 Have Broad-Spectrum Antiviral Activity against Coronaviruses. ACS Infect. Dis. 2021, 7 (3), 586–597. [PubMed: 33645977]
21. Hoffman RL; Kania RS; Brothers MA; Davies JF; Ferre RA; Gajiwala KS; He M; Hogan RJ; Kozminski K; Li LY; Lockner JW; Lou J; Marra MT; Mitchell LJ; Murray BW; Nieman JA; Noell S; Planken SP; Rowe T; Ryan K; Smith GJ; Solowiej JE; Stepan CM; Taggart B, Discovery of Ketone-Based Covalent Inhibitors of Coronavirus 3CL Proteases for the Potential Therapeutic Treatment of COVID-19. J. Med. Chem. 2020, 63 (21), 12725–12747. [PubMed: 33054210]
22. Rathnayake AD; Zheng J; Kim Y; Perera KD; Mackin S; Meyerholz DK; Kashipathy MM; Battaile KP; Lovell S; Perlman S; Groutas WC; Chang K-O, 3C-like protease inhibitors block coronavirus replication in vitro and improve survival in MERS-CoV-infected mice. Sc. Transl. Med. 2020, 12 (557), eabc5332. [PubMed: 32747425]
23. Dai W; Zhang B; Jiang X-M; Su H; Li J; Zhao Y; Xie X; Jin Z; Peng J; Liu F; Li C; Li Y; Bai F; Wang H; Cheng X; Cen X; Hu S; Yang X; Wang J; Liu X; Xiao G; Jiang H; Rao Z; Zhang L-K; Xu Y; Yang H; Liu H, Structure-based design of antiviral drug candidates targeting the SARS-CoV-2 main protease. Science 2020, 368 (6497), 1331–1335. [PubMed: 32321856]
24. Kitamura N; Sacco MD; Ma C; Hu Y; Townsend JA; Meng X; Zhang F; Zhang X; Ba M; Szeto T; Kukuljac A; Marty MT; Schultz D; Cherry S; Xiang Y; Chen Y; Wang J, Expedited Approach toward the Rational Design of Noncovalent SARS-CoV-2 Main Protease Inhibitors. J. Med. Chem. 2021, doi: 10.1021/acs.jmedchem.1c00509.
25. Jacobs J; Grum-Tokars V; Zhou Y; Turlington M; Saldanha SA; Chase P; Egger A; Dawson ES; Baez-Santos YM; Tomar S; Mielech AM; Baker SC; Lindsley CW; Hodder P; Mesecar A; Stauffer SR, Discovery, synthesis, and structure-based optimization of a series of N-(tert-butyl)-2-(N-arylamido)-2-(pyridin-3-yl) acetamides (ML188) as potent noncovalent small molecule inhibitors of the severe acute respiratory syndrome coronavirus (SARS-CoV) 3CL protease. J. Med. Chem. 2013, 56 (2), 534–546. [PubMed: 23231439]
26. Abdeldayem A; Raouf YS; Constantinescu SN; Moriggl R; Gunning PT, Advances in covalent kinase inhibitors. Chem. Soc. Rev. 2020, 49 (9), 2617–2687. [PubMed: 32227030]
27. Siklos M; BenAissa M; Thatcher GR, Cysteine proteases as therapeutic targets: does selectivity matter? A systematic review of calpain and cathepsin inhibitors. Acta Pharm. Sin. B 2015, 5 (6), 506–519. [PubMed: 26713267]
28. Cianni L; Feldmann CW; Gilberg E; Gutschow M; Juliano L; Leitao A; Bajorath J; Montanari CA, Can Cysteine Protease Cross-Class Inhibitors Achieve Selectivity? J. Med. Chem. 2019, 62 (23), 10497–10525. [PubMed: 31361135]
29. Hoch DG; Abegg D; Adibekian A, Cysteine-reactive probes and their use in chemical proteomics. Chem. Commun. 2018, 54 (36), 4501–4512.

30. Le GT; Abbenante G; Madala PK; Hoang HN; Fairlie DP, Organic Azide Inhibitors of Cysteine Proteases. *J. Am. Chem. Soc.* 2006, 128 (38), 12396–12397. [PubMed: 16984172]
31. Yang P-Y; Wu H; Lee MY; Xu A; Srinivasan R; Yao SQ, Solid-Phase Synthesis of Azidomethylene Inhibitors Targeting Cysteine Proteases. *Org. Lett.* 2008, 10 (10), 1881–1884. [PubMed: 18407644]
32. Thorarensen A; Balbo P; Banker ME; Czerwinski RM; Kuhn M; Maurer TS; Telliez J-B; Vincent F; Wittwer AJ, The advantages of describing covalent inhibitor in vitro potencies by IC50 at a fixed time point. IC50 determination of covalent inhibitors provides meaningful data to medicinal chemistry for SAR optimization. *Bioorg. Med. Chem.* 2021, 29, 115865. [PubMed: 33285410]
33. Drayman N; DeMarco JK; Jones KA; Azizi S-A; Froggatt HM; Tan K; Maltseva NI; Chen S; Nicolaescu V; Dvorkin S; Furlong K; Kathayat RS; Firpo MR; Mastrodomenico V; Bruce EA; Schmidt MM; Jedrzejczak R; Muñoz-Alfía MÁ; Schuster B; Nair V; Han K.-y.; O’Brie A.; Tomatsidou A; Meyer B; Vignuzzi M; Missiakas D; Botten JW; Brooke CB; Lee H; Baker SC; Mounce BC; Heaton NS; Severson WE; Palmer KE; Dickinson BC; Joachimiak A; Randall G; Tay S, Masitinib is a broad coronavirus 3CL inhibitor that blocks replication of SARS-CoV-2. *Science* 2021, 373 (6557), 931–936. [PubMed: 34285133]
34. Hoffmann M; Kleine-Weber H; Schroeder S; Kruger N; Herrler T; Erichsen S; Schiergens TS; Herrler G; Wu NH; Nitsche A; Muller MA; Drosten C; Pohlmann S, SARS-CoV-2 Cell Entry Depends on ACE2 and TMPRSS2 and Is Blocked by a Clinically Proven Protease Inhibitor. *Cell* 2020, 181 (2), 271–280 e8. [PubMed: 32142651]
35. Bertram S; Glowacka I; Blazejewska P; Soilleux E; Allen P; Danisch S; Steffen I; Choi SY; Park Y; Schneider H; Schughart K; Pohlmann S, TMPRSS2 and TMPRSS4 facilitate trypsin-independent spread of influenza virus in Caco-2 cells. *J. Virol.* 2010, 84 (19), 10016–25. [PubMed: 20631123]
36. Stanifer ML; Kee C; Cortese M; Zumaran CM; Triana S; Mukenhirn M; Kraeusslich HG; Alexandrov T; Bartenschlager R; Boulant S, Critical Role of Type III Interferon in Controlling SARS-CoV-2 Infection in Human Intestinal Epithelial Cells. *Cell Rep.* 2020, 32 (1), 107863. [PubMed: 32610043]
37. Shang J; Wan Y; Luo C; Ye G; Geng Q; Auerbach A; Li F, Cell entry mechanisms of SARS-CoV-2. *Proc. Natl. Acad. Sci. U. S. A.* 2020, 117 (21), 11727–11734. [PubMed: 32376634]
38. Gunther S; Reinke PYA; Fernandez-Garcia Y; Lieske J; Lane TJ; Ginn HM; Koua FHM; Ehrst C; Ewert W; Oberthuer D; Yefanov O; Meier S; Lorenzen K; Krichel B; Kopicki JD; Gelisio L; Brehm W; Dunkel I; Seychell B; Gieseler H; Norton-Baker B; Escudero-Perez B; Domaracky M; Saouane S; Tolstikova A; White TA; Hanle A; Groessler M; Fleckenstein H; Trost F; Galchenkova M; Gevorkov Y; Li C; Awel S; Peck A; Barthelmess M; Schlunzen F; Lourdu Xavier P; Werner N; Andaleeb H; Ullah N; Falke S; Srinivasan V; Franca BA; Schwinzer M; Brognaro H; Rogers C; Melo D; Zaitseva-Doyle JJ; Knoska J; Pena-Murillo GE; Mashhour AR; Hennicke V; Fischer P; Hakanpaa J; Meyer J; Gribbon P; Ellinger B; Kuzikov M; Wolf M; Beccari AR; Bourenkov G; von Stetten D; Pompidor G; Bento I; Panneerselvam S; Karpics I; Schneider TR; Garcia-Alai MM; Niebling S; Gunther C; Schmidt C; Schubert R; Han H; Boger J; Monteiro DCF; Zhang L; Sun X; Pletzer-Zelgert J; Wollenhaupt J; Feiler CG; Weiss MS; Schulz EC; Mehrabi P; Karnicar K; Usenik A; Loboda J; Tidow H; Chari A; Hilgenfeld R; Utrecht C; Cox R; Zaliani A; Beck T; Rarey M; Gunther S; Turk D; Hinrichs W; Chapman HN; Pearson AR; Betzel C; Meents A, X-ray screening identifies active site and allosteric inhibitors of SARS-CoV-2 main protease. *Science* 2021, 372 (6542), 642–646. [PubMed: 33811162]
39. Douangamath A; Fearon D; Gehrtz P; Krojer T; Lukacik P; Owen CD; Resnick E; Strain-Damerell C; Aimon A; Ábrányi-Balogh P; Brandão-Neto J; Carbery A; Davison G; Dias A; Downes TD; Dunnett L; Fairhead M; Firth JD; Jones SP; Keeley A; Keserü GM; Klein HF; Martin MP; Noble MEM; O’Brien P; Powell A; Reddi RN; Skyner R; Snee M; Waring MJ; Wild C; London N; von Delft F; Walsh MA, Crystallographic and electrophilic fragment screening of the SARS-CoV-2 main protease. *Nat. Commun.* 2020, 11 (1), 5047. [PubMed: 33028810]
40. Huang C; Wei P; Fan K; Liu Y; Lai L, 3C-like Proteinase from SARS Coronavirus Catalyzes Substrate Hydrolysis by a General Base Mechanism. *Biochemistry* 2004, 43 (15), 4568–4574. [PubMed: 15078103]

41. Verma N; Henderson JA; Shen J, Proton-Coupled Conformational Activation of SARS Coronavirus Main Proteases and Opportunity for Designing Small-Molecule Broad-Spectrum Targeted Covalent Inhibitors. *J. Am. Chem. Soc.* 2020, 142 (52), 21883–21890. [PubMed: 33320670]

Author Manuscript

Author Manuscript

Author Manuscript

Author Manuscript

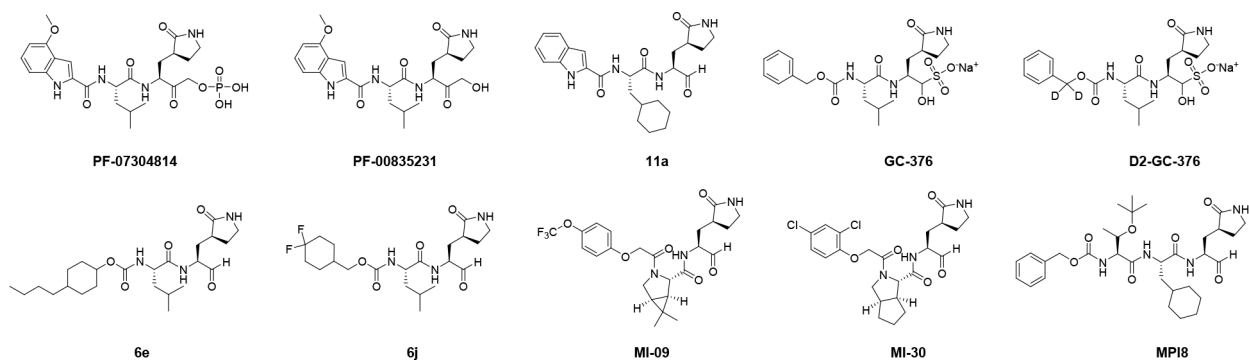


Figure 1.
Advanced SARS-CoV-2 M^{pro} inhibitors with translational potential.

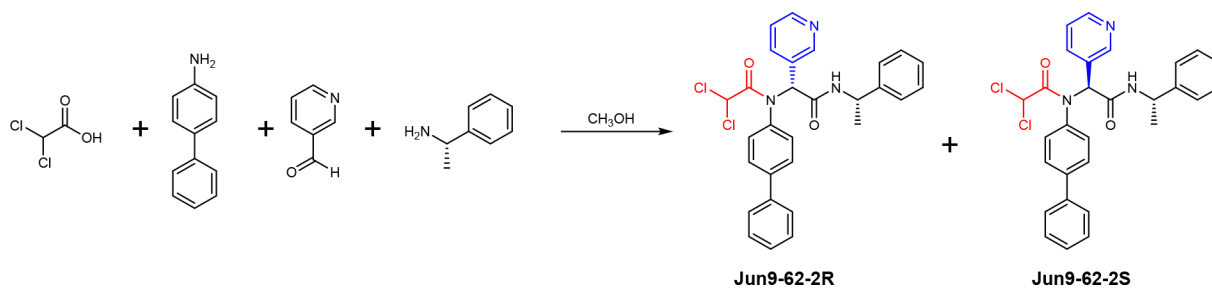
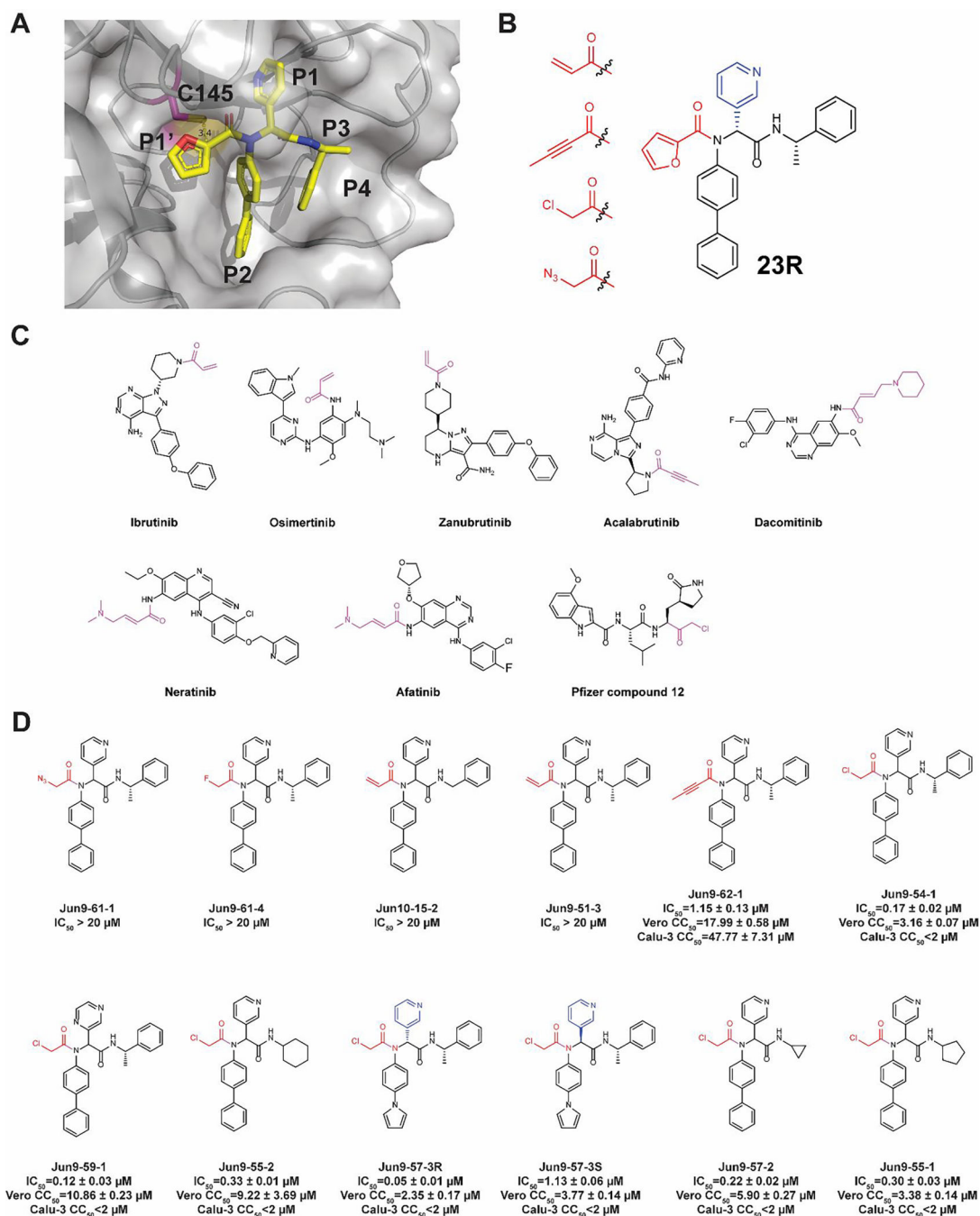


Figure 2. Synthesis route for the covalent SARS-CoV-2 M^{Pro} inhibitors through Ugi-4CR. The R and S chirality refers to the chiral center at the pyridine substitution.

**Figure 3.**

Rational design of covalent SARS-CoV-2 M^{Pro} inhibitors based on **23R**. (A) X-ray crystal structure of SARS-CoV-2 M^{Pro} with **23R** (PDB: 7KX5). The distance between the furin ring and the catalytic cysteine 145 is 3.4 Å. (B) Representative cysteine reactive warheads for covalent labeling of C145. (C) FDA-approved covalent inhibitors. The reactive warheads are colored in magenta. Pfizer compound **12** is a preclinical candidate. (D) Designed covalent SARS-CoV-2 M^{Pro} inhibitors. The results are average ± standard deviation of three repeats.

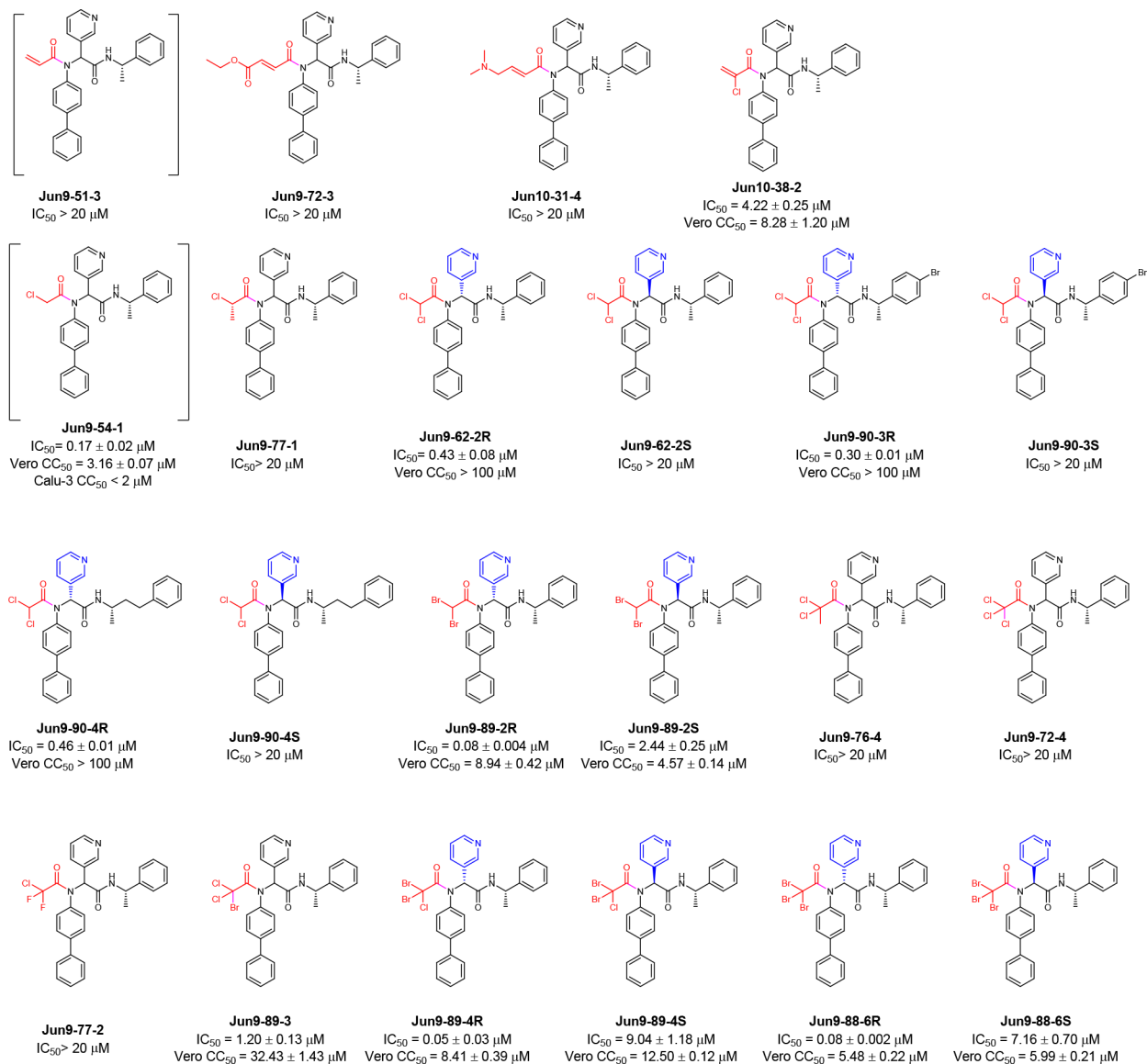


Figure 4. SARS-CoV-2 M^{pro} inhibitors with novel acrylamide and haloacetamide warheads. The results are average ± standard deviation of three repeats.

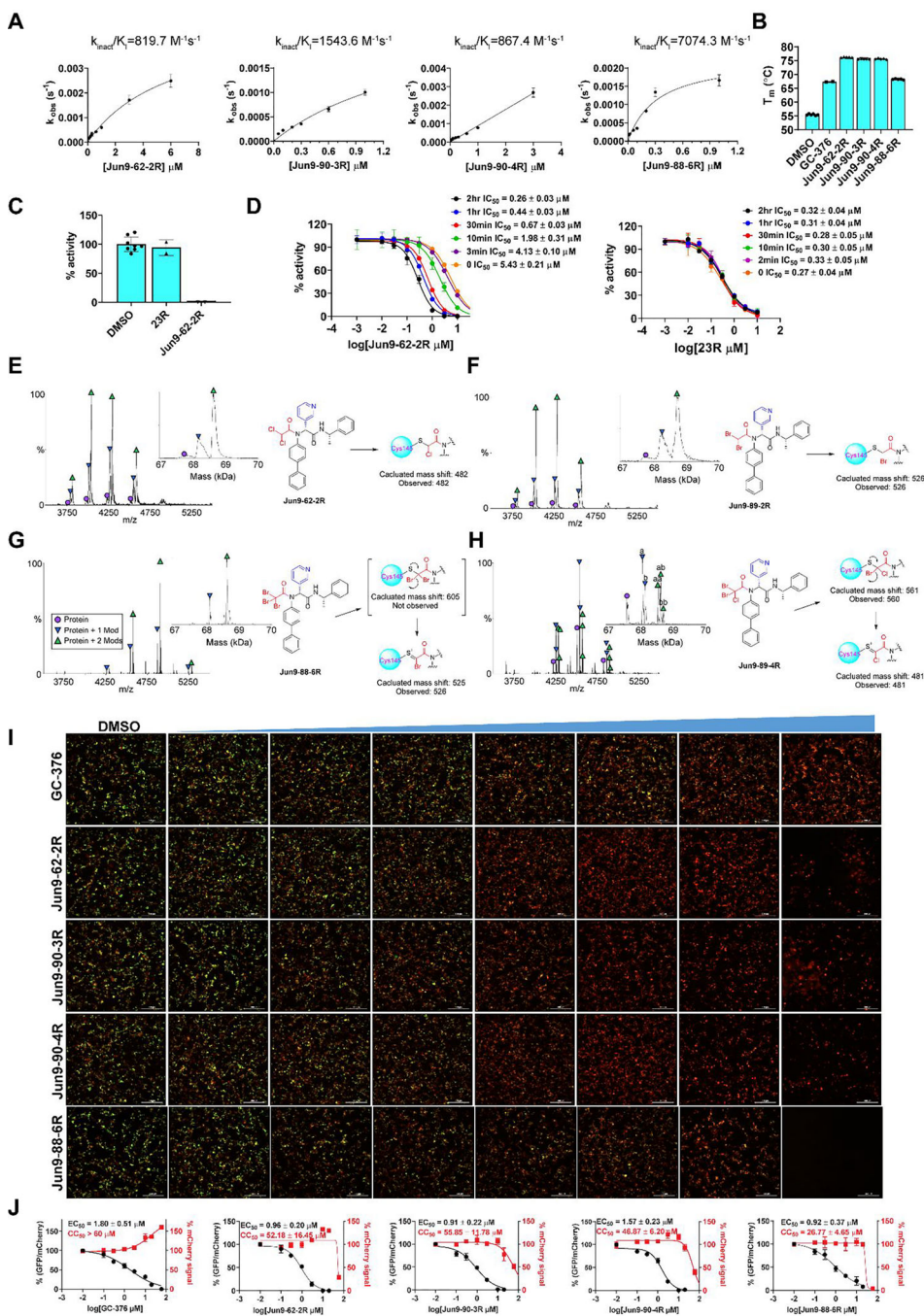


Figure 5. Pharmacological characterization of the SARS-CoV-2 M^{Pro} inhibitors. (A) Curve fittings of the enzymatic kinetic studies of four compounds **Jun9-62-2R**, **Jun9-90-3R**, **Jun9-90-4R**, and **Jun9-88-6R** against SARS-CoV-2 M^{Pro}. (B) Binding of four compounds **Jun9-62-2R**, **Jun9-90-3R**, **Jun9-90-4R**, and **Jun9-88-6R** to SARS-CoV-2 M^{Pro} in the thermal shift assay. (C) Fast dilution experiment. 10 μM M^{Pro} was pre-incubated with 10 μM of testing compounds for 2 h at 30 °C; the pre-formed compound-enzyme complex was diluted 100-fold into reaction buffer before initiate the enzymatic reaction. The recovered enzymatic

activity was compared with DMSO control. **23R** is a non-covalent M^{PRO} inhibitor and it was included as a control. (D) Time dependent inhibition of M^{PRO} by **Jun9-62-2R**. 100 nM SARS CoV-2 M^{PRO} was pre-incubated with **Jun9-62-2R** for various period of time (0 min to 2 h) before the addition of 10 μ M FRET substrate to initiate the enzymatic reaction. **23R** was included as a control. (E-H) Native mass spectrometry assay of SARS-CoV-2 M^{PRO} reveals binding of **Jun9-62-2R** with mass modifications of 482 Da (E), **Jun9-89-2R** with mass modifications of 526 Da (F), **Jun9-88-6R** with mass modifications of 526 Da (G), and **Jun9-89-4R** with mass modifications of (a) 481 and (b) 561 Da (H). M^{PRO} functions as a dimer, and both one drug per dimer (Protein + 1 Mod) and two drugs per dimer (Protein + 2 Mods) were observed. (I) FlipGFP assay characterization of the inhibition of the cellular enzymatic activity of SARS-CoV-2 M^{PRO} by the four compounds **Jun9-62-2R**, **Jun9-90-3R**, **Jun9-90-4R**, and **Jun9-88-6R**. (J) Curve fittings of the FlipGFP M^{PRO} assay. The results are average \pm standard deviation of three repeats.

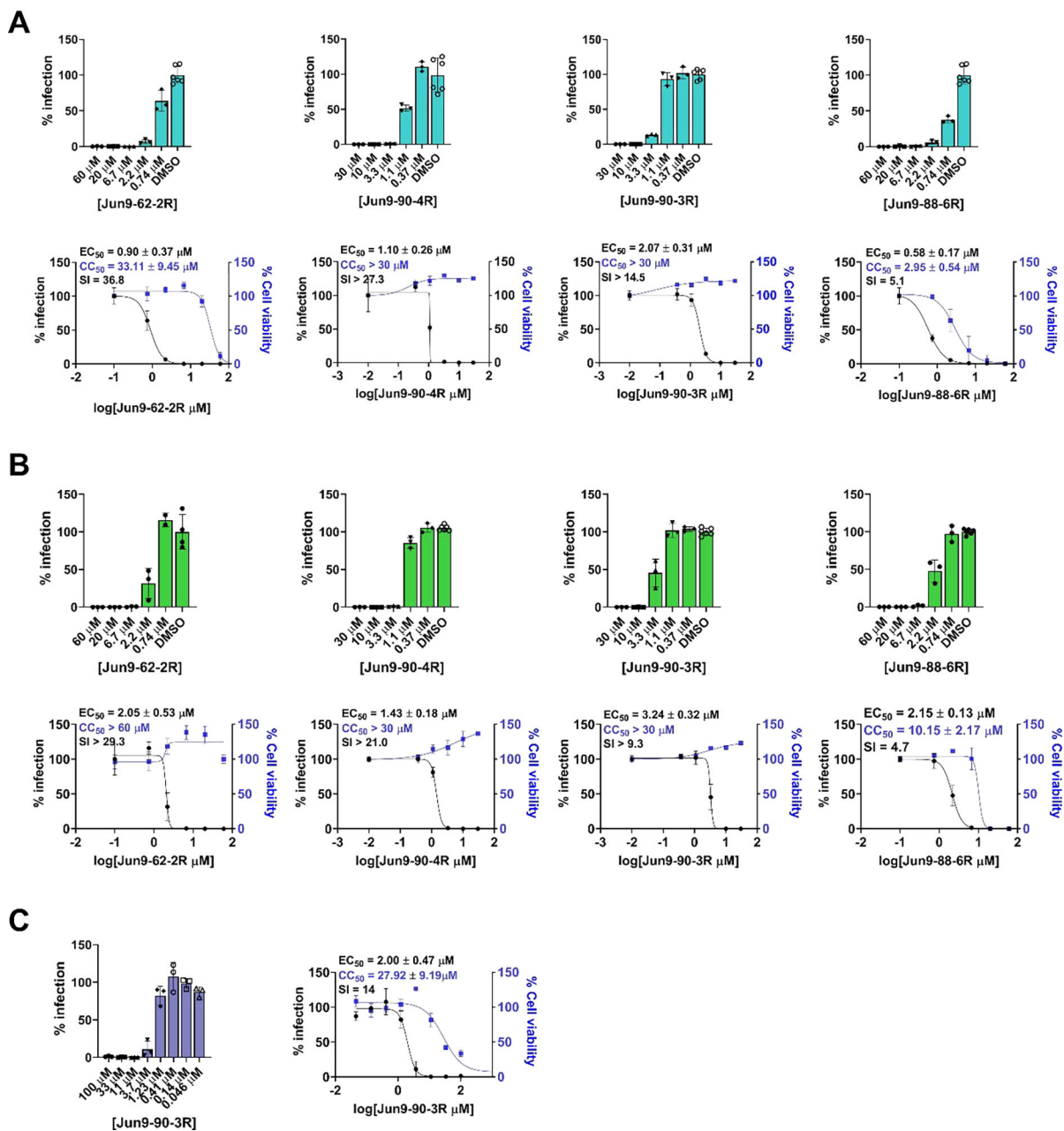
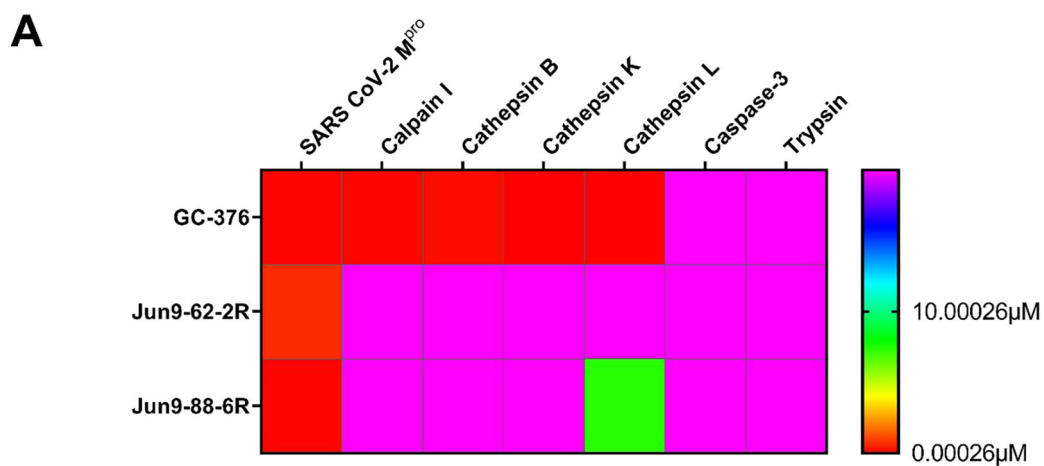


Figure 6. Antiviral activity of **Jun9-62-2R**, **Jun9-90-3R**, **Jun9-90-4R**, and **Jun9-88-6R** against SARS-CoV-2 in different cell lines. (A) Antiviral activity against SARS-CoV-2 in Vero E6 cells. (B) Antiviral activity against SARS-CoV-2 in Caco2-hACE2 cells. (C) Antiviral activity of **Jun9-90-3R** in Calu-3 cells. The results are average ± standard deviation of three repeats.



B

Compound	SARS CoV-2 M ^{pro}	SARS CoV M ^{pro}	Calpain I	Cathepsin B	Cathepsin K	Cathepsin L	Caspase-3	Trypsin
	IC ₅₀ (μM)							
GC-376	0.037 ± 0.002	0.079 ± 0.006 ^a	0.074 ± 0.016	0.16 ± 0.01	0.00026 ± 0.00004	0.0027 ± 0.0009	>20	>20
Jun9-62-2R	0.67 ± 0.07	1.01 ± 0.21	>20	>20	>20	>20	>20	>20
Jun9-88-6R	0.078 ± 0.002	0.31 ± 0.04	>20	>20	>20	7.37 ± 1.02	>20	>20

Figure 7.

Target selectivity of SARS-CoV-2 M^{pro} inhibitors against host proteases. (A) Heat map of target selectivity. (B) IC₅₀ values of **Jun9-62-2R** and **Jun9-88-6R** against host proteases in the FRET-based enzymatic assay. ^aThe result was from reference²⁰

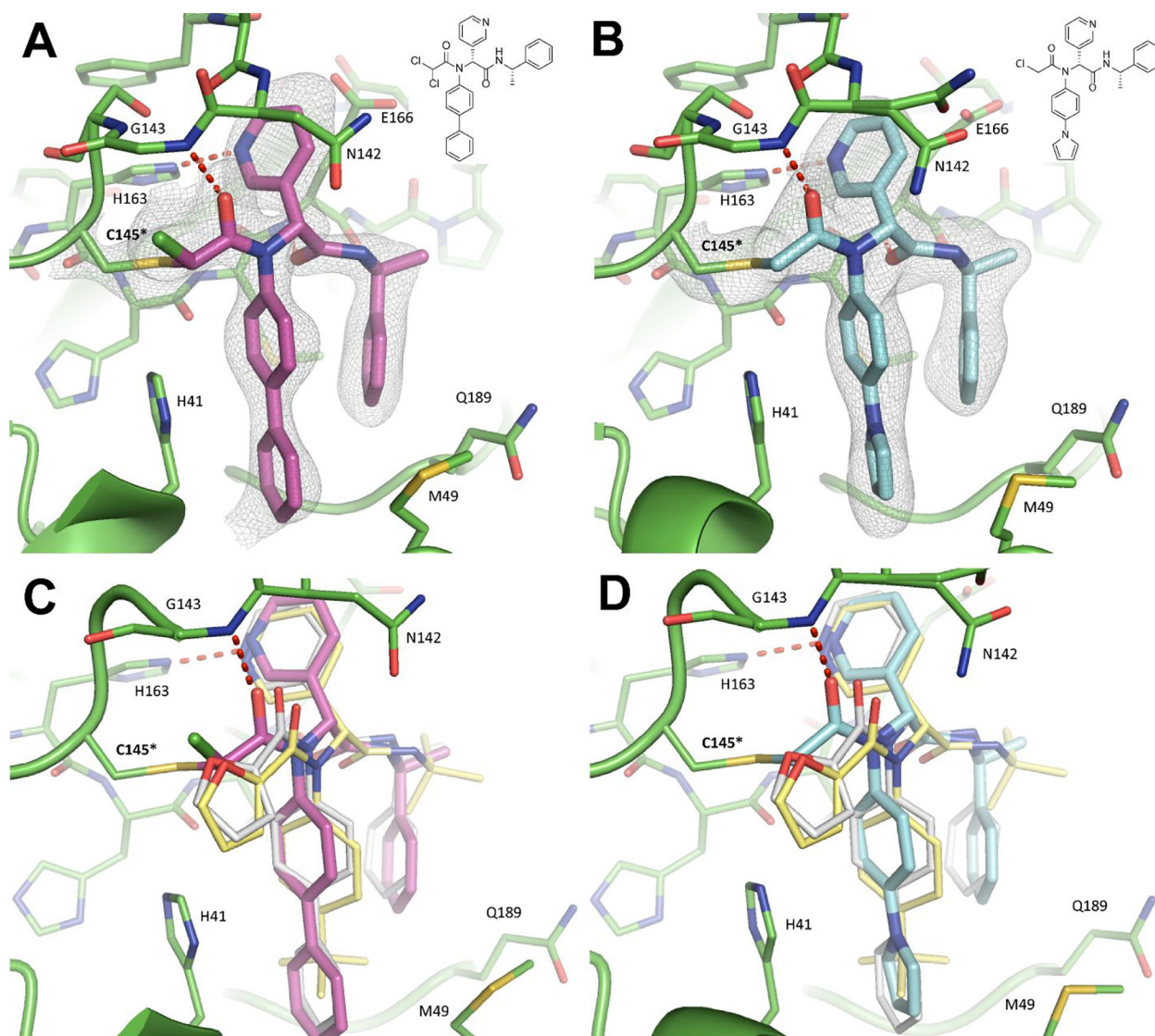


Figure 8. X-ray crystal structures of SARS-CoV-2 M^{Pro} in complex with **Jun9-62-2R** (A) and **Jun9-57-3R** (B). 2Fo-Fc electron density map, shown in gray, is contoured at 1σ. Structural superimposition of the noncovalent analogues **Jun8-76-3A** (white, PDB ID 7KX5) and **ML188** (yellow, PDB ID 7L0D) with **Jun9-62-2R** (C) and **Jun9-57-3R** (D) reveal a different mode of interaction with the catalytic core.

Table 1.Target specificity of SARS-CoV-2 M^{PRO} inhibitors.

Compound	SARS-CoV-2 M ^{PRO} IC ₅₀ (nM)	Cathepsin L IC ₅₀ (nM)	Additional off targets	References
GC-376	33	0.99	Calpain I (IC ₅₀ = 74 nM) Cathepsin K (IC ₅₀ = 0.56 nM)	8, 17–18, 20, 24
MPI8	105	1.2	Cathepsin B (IC ₅₀ = 230 nM) Cathepsin K (IC ₅₀ = 180 nM)	15–16
PF-00835231	5	146	Cathepsin B (IC ₅₀ = 1.3 μM)	19, 21
6e	10	< 0.5	-	19, 22
6j	7	< 0.5	-	19, 22
11a	8	0.21	-	19, 23